BUTTERWORTH HEINEMANN

Polymer Vol. 36 No. 9, pp. 1809–1815, 1995

0032-3861/95/$10.00 + 0.00

The microstructure of the poly(ethylene oxide)/sodium dodecyl sulfate system studied by cryogenic-temperature transmission electron microscopy and small-angle X-ray scattering*

Dorit Süss, Yachin Cohen and Yeshayahu Talmon†
Department of Chemical Engineering, Technion–Israel Institute of Technology, Haifa 32000, Israel

The microstructure of semidilute mixed solutions of poly(ethylene oxide) (PEO) and sodium dodecyl sulfate (SDS) was characterized by the combination of cryogenic-temperature transmission electron microscopy (cryo-TEM) and small-angle X-ray scattering (SAXS). Cryo-TEM provides direct images that elucidate the basic microstructural building blocks of the system, with which an accurate physical model can be constructed for scattering data interpretation. SAXS then provides the desired quantitative information, which is not accurately available from microscopy. This experimental approach has been most successful in proving the existence of thread-like SDS micelles in the presence of high NaCl concentration, and their transformation to spheroidal micelles upon polymer addition. Preliminary data on a more strongly interacting system, namely gelatin/SDS, are also presented.

(Keywords: SAXS; cryo-TEM; polymer/surfactant interaction)

INTRODUCTION

Polymer/surfactant interactions in solution are affected by three major factors: (a) polymer/solvent interactions, which manifest themselves in the configuration of the polymer coil; (b) surfactant/solvent interactions, which affect self-aggregation of the surfactant in solution; and (c) interactions between a single surfactant molecule and a single polymer building unit[1].

In the case of a solution of a non-ionic polymer and an ionic surfactant, the interactions are rather weak, and are probably hydrophobic in nature. Single molecules and small surfactant aggregates attach themselves to the polymer chain. A 'critical aggregation concentration' (*CAC*), analogous to the critical micellization concentration (*CMC*), has been defined. It corresponds to the surfactant concentration at which aggregation on the polymer molecule starts; it is typically much lower than *CMC* in pure water. This process of aggregation continues until the polymer molecule is saturated with those aggregates. At concentrations higher than saturation, free micelles are formed in solution[1,2].

A polymer and a surfactant of opposing charges interact strongly, forming surfactant aggregates that are bound electrostatically to the polymer coil. This interaction starts at very low surfactant concentration for a given polymer concentration, typically several orders of magnitude lower than the *CMC*[3]. As the surfactant concentration is increased, sedimentation takes place, possibly due to the formation of electrostatically balanced aggregates[4]. At excess surfactant, those aggregates are eventually solubilized.

Although until recently it was the accepted belief that a charged surfactant would not interact with a polyelectrolyte of like charge, more recent evidence[5,6] indicates that this is not the case when the charged polymer is either sufficiently hydrophobic or made so by chemical modification.

Almost all the data available in the literature on polymer/surfactant systems come from experimental techniques that are model-dependent, i.e. require a preconceived model for data interpretation. To obtain a more complete picture of polymer/surfactant interactions, we have applied in this work our experimental approach of combining direct imaging by cryogenic-temperature transmission electron microscopy (cryo-TEM) with an indirect but more quantitative method, in this case small-angle X-ray scattering (SAXS)—see for example Burns *et al.*[7]. Microscopy gives direct images of the structural elements of the system under investigation, but, in general, is not a very quantitative tool. Microscopical data interpretation is limited by factors such as superposition, calibration inaccuracies and redistribution of material in the sample during its preparation. SAXS, however, like other scattering techniques, gives accurate quantitative data, but their interpretation is model-dependent, and thus non-unique. The results from microscopy, then, are used to construct a dependable,

* Presented at 'Aspects of Imaging in Polymer Science', 51st Annual Meeting of the Microscopy Society of America, 1–6 August 1993, Cincinnati, OH, USA

† To whom correspondence should be addressed

unique physical model, which is used to analyse the SAXS data, thus giving a complete microstructural picture of the investigated system.

We have focused our attention on the poly(ethylene oxide)/sodium dodecyl sulfate (PEO/SDS) system. This is a well studied system, with much information available from indirect techniques. The present work is, however, the first example of applying our experimental approach to a polymer/surfactant system.

The phase diagram of the PEO/SDS system at low concentration of polymer and surfactant was mapped[1] from data obtained by measuring dye solubilization[8], electrical conductivity[9] and interfacial tension[10]. More recently, viscosity data have been added to the literature[11]. This phase diagram is divided into three regions by two lines: one, denoted X_1, corresponds to the critical aggregation concentration (*CAC*), and the other, denoted X_2, corresponds to saturating the polymer chain with adsorbed surfactant molecules. The X_1 line is almost perpendicular, i.e. the *CAC* is a very weak function of polymer concentration. These lines define a region of no surfactant aggregation (region I), a region of excess polymer (region II) and a region of excess surfactant (region III). The existence of another line, X'_2, has been postulated. Cabane and Duplessix[1] suggested that free DS^- ions exist in the narrow region between lines X_2 and X'_2.

The first model of PEO/SDS interactions[12] envisioned the surfactant molecules adsorbed individually onto the polymer chain. That model failed to explain the existence of *CAC*, and the lack of interaction between SDS and PEO with molecular weight lower than 2000. The aggregate concept emerged first from n.m.r. results[10]. The full model was constructed later by Cabane and Duplessix[1], based on their n.m.r. and small-angle neutron scattering data. The model suggests that the polymer chain engulfs the surfactant aggregate. Only a limited number of monomer units can adsorb onto one surfactant aggregate. As the number of aggregates grows upon increasing the surfactant concentration, the electrostatic interaction between them grows, giving rise to an increase in polymer coil volume, and thus to increase in the viscosity of the system[11].

Based on fluorescence techniques, it was suggested by van Stam *et al.*[13] that, at low polymer concentrations, all the aggregation sites on the polymer chains are occupied simultaneously at the *CAC*, with an initial aggregation number about one-third of that at the SDS *CMC*. In the semidilute region new aggregates are formed as more surfactant is added. Zana *et al.*[14] found that the surfactant aggregates are smaller than free SDS micelles. The aggregation number was found to decrease, and the degree of ionization to increase, with increased polymer or decreased surfactant concentration.

A non-ionic polymer with a molecular weight lower than a critical value does not interact appreciably with an ionic surfactant. Above that critical value, the molecular weight does not have any noticeable effect on the polymer/surfactant interaction. Brackman and Engberts[15] found that critical value to be about 4000 for the PEO/SDS system.

The addition of salt has a pronounced effect on the aggregation pattern of the surfactant. At NaCl concentration higher than 0.4 M, SDS forms thread-like micelles; the system needs to be kept at elevated temperature of about 40°C to prevent precipitation. Cabane and Duplessix[1] examined PEO/SDS solutions up to a NaCl concentration of 0.8 M, and found for that entire concentration range that the surfactant aggregated into spheroidal, not thread-like, aggregates. The polymer seems to counteract the screening effect of the salt, which allows the head-groups to come closer together, thus making packing into larger aggregates possible. The aggregation number in the presence of electrolyte was found to increase. The number of aggregates per given length of polymer molecule was also found to increase upon salt addition.

The cryo-TEM and SAXS work we describe in this paper addresses the issues of the effects of PEO on SDS aggregation with and without the presence of salt.

MATERIALS AND METHODS

Materials

Sodium dodecyl sulfate (SDS) (BDH, specially pure) and poly(ethylene oxide) (PEO) (Aldrich, weight-average molecular weight 100 000) were used as received. Gelatin (deionized photographic gelatin manufactured by Eastman Gel, Peabody, MA) was kindly supplied by Dr J. Minter of the Eastman Kodak Co. PEO solutions were prepared by heating to 50°C for 1 h with stirring, to ensure that the polymer molecules are not trapped in microgels or microcrystallites[1]. All polymer solutions were beyond the polymer crossover concentration.

Electron microscopy

Vitrified specimens for cryo-TEM were prepared in a controlled-environment vitrification system (CEVS), as described by Bellare *et al.*[16]. Most specimens were prepared at room temperature, while some, those containing high salt concentration, were prepared at 40°C. All specimens were prepared at relative humidity close to 100%. Specimen preparation was carried out by applying a small drop of the solution (ca. 3 μl) onto a TEM copper grid covered with a perforated carbon film (hole diameter from 1 to 10 μm), held by tweezers inside the CEVS. Most of the drop was blotted away, leaving behind thin liquid films (ideally 50 to 200 nm thick) spanning the holes of the support film. All sample manipulations were performed from outside the chamber through a pair of rubber septa. Upon triggering of the release mechanism, the tweezer holding the sample was propelled into liquid ethane at its freezing point, thus assuming ultra-high cooling rates, sufficient for water vitrification. The working assumption is that if water is prevented from rearranging into a crystalline ice, the larger polymer and surfactant molecules are not rearranged either.

The vitrified specimen is transferred from the ethane into liquid nitrogen, and subsequently into the cryogenic specimen holder, seated in its 'work-station' (both from Gatan, model 626). The holder is inserted into the microscope (JEOL 2000FX and Philips CM12 microscopes were used in this work), thus completing the transfer of specimen with minimal heating and frost deposition. After allowing the specimens to equilibrate thermally in the microscope, they were examined at an acceleration voltage of 100 kV, using low-dose procedures to minimize electron-beam radiation damage. Images were recorded by 1 s exposure of Kodak SO163 electron

film. Negatives were developed in full-strength Kodak D-19 for 12 min to achieve maximum film speed.

Small-angle X-ray scattering (SAXS)

SAXS measurements were performed with a Ni-filtered Cu Kα radiation with a compact Kratky camera having a temperature-controlled sample holder (A. Paar Co.) and a linear position-sensitive detector system (Raytech). The entrance slit to the collimation block was 40 μm, and the length limiting slits were set at 15 mm. Sample-to-detector distance was 26.4 cm. Samples were placed in cylindrical quartz cells (A. Paar, 1 mm path length). The background scattering was measured for an SDS solution at the *CMC*, whose scattering curve was found to be essentially identical to that of pure water. For scattering from the complex solutions, a PEO solution of the same polymer concentration was used as background. To prevent small deviations in the scattered intensity, the curves were normalized to the tail of the background scattering curve at $h > 4\,\mathrm{nm}^{-1}$ ($h = 4\pi \sin\theta/\lambda$, where 2θ is the scattering angle and λ the wavelength), and the background was subtracted.

Model calculation of scattering curves

The scattering curves were analysed by comparing the experimental data to simulated ones. The simulation of spherical micelles was based on a hollow-sphere form factor[17]:

$$I(h) = n_s(\tfrac{4}{3}\pi)^2[(B_2 - B_1)R_1^3 f(R_1 h) - (B_2 - B_s)R_2^3 f(R_2 h)]^2 \quad (1)$$

where

$$f(x) = 3[\sin(x) - x\cos(x)]/x^3 \quad (2)$$

B_1, B_2 and B_s are the electron densities of the hydrophobic core, the ionic shell and the solvent, respectively, R_1 is the radius of the hydrophobic core, R_2 is the radius of the whole micelle and n_s is the number of micelles per unit volume.

The model calculation of cylindrical micelles was based on a hollow-cylinder form factor[18]:

$$I(h) = n_s L(\pi/h) P_c^2(h) \quad (3)$$

where

$$P_c(\mathrm{h}) = \frac{2J_2(R_2 h)}{R_2 h} - \left(\frac{R_1}{R_2}\right)^3 \left(\frac{B_2 - B_1}{B_2 - B_s}\right) \frac{2J_1(R_1 h)}{R_1 h} \quad (4)$$

in which J_1 is the first-order Bessel function and L is the cylinder length. Equations (1)–(4) are valid for scattering from a pinhole-collimated incident beam. In order to adjust the simulated curves to the conditions of slit collimation, the smeared intensity of the model was calculated as[19]:

$$\tilde{I}(h) = 2\int_0^\infty M(t) I((h^2 + t^2)^{1/2})\,\mathrm{d}t \quad (5)$$

where $M(t)$ is the length profile of the incident beam measured at the detector plane.

The simulated scattering patterns were calculated using equations (1), (2) and (5) for spherical micelles, and equations (3)–(5) for cylindrical micelles. Electron density values were given by Zemb and Charpin[17]: $B_1 = 0.280$, $B_2 = 0.445$ and $B_s = 0.330\,\mathrm{e}^-\,\text{Å}^{-3}$. There were, thus, three parameters to be fitted: the diameter of the micelle ($2R_2$), the thickness of the ionic corona ($R_2 - R_1$), and a scaling factor for the intensity. These parameters were evaluated by fitting the position and breadth of the intramicellar scattering peak due to the electron-rich corona of the head-group region. The diameter and corona thickness were altered in steps of 0.1 nm, until the peak position and breadth matched the experimental data. The scaling factor was set to match the peak height.

RESULTS

Small-angle X-ray scattering (SAXS) curves of micellar solutions of SDS reveal one distinct peak that corresponds to the micelle electron-rich 'corona' of the surfactant head-groups (peak a in *Figure 1*). That peak is absent in solutions below the critical micelle concentration (*CMC*, about 8.4 mM or 0.22 wt% for SDS), and becomes stronger with increasing surfactant concentration. A second peak, attributed to intermicellar interactions[17], appears at higher SDS concentrations (peak b in *Figure 1*). Electron micrographs of SDS solutions above the *CMC* show the projection of many spheroidal micelles (*Figure 2*). PEO itself is transparent to the electron beam because of lack of contrast with respect to water.

In the presence of PEO the micelles are still spheroidal, as is revealed by cryo-TEM (*Figure 3*). It is very difficult

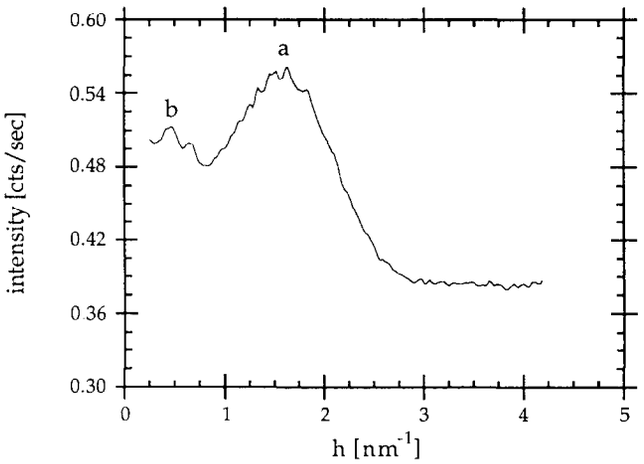

Figure 1 Scattering curve of spheroidal SDS micelles in 2 wt% SDS solution: (a) the intramicellar peak; (b) the intermicellar peak

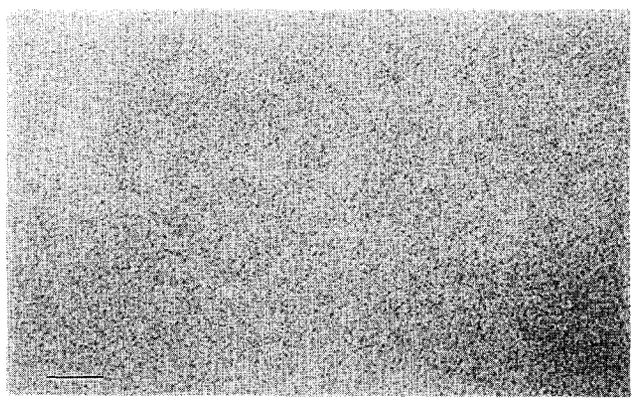

Figure 2 Cryo-TEM image of a 3 wt% aqueous SDS solution. Small dark globules are SDS micelles (scale bar = 100 nm)

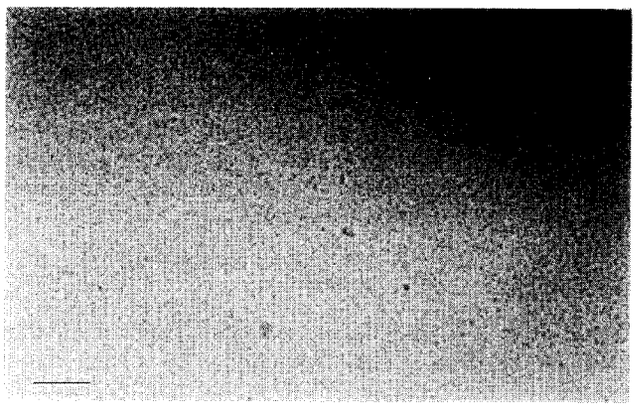

Figure 3 An electron micrograph of a vitrified specimen of 1 wt% PEO/2 wt% SDS: globular micelles are clearly visible (scale bar = 100 nm)

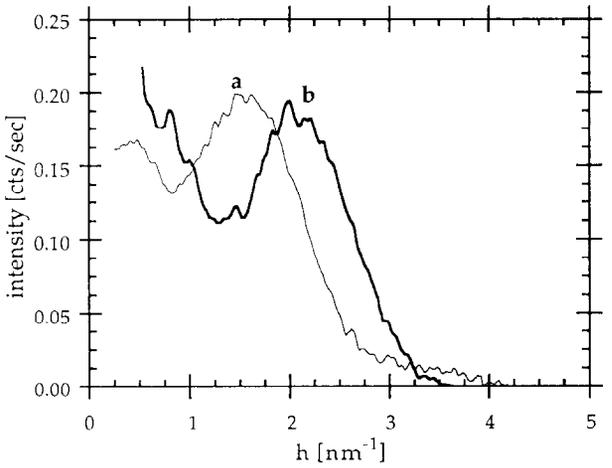

Figure 4 SAXS curves: (a) 2 wt% SDS; (b) 1 wt% PEO/2 wt% SDS solution

to assess any size changes by comparing this micrograph to that of *Figure 2*. But micrographs such as this do demonstrate that the micelles are still spheroidal, and of comparable size to those in the absence of the polymer. Quantitative information is provided by SAXS (*Figure 4*). The scattering curve in the presence of the polymer (curve b in *Figure 4*) shows reduction in micellar size relative to SDS in water alone (curve a). Modelling of these scattering curves has been undertaken to improve the quantitative evaluation of the micelle dimension. *Figure 5* shows a comparison between an experimental scattering curve and a calculated curve (thicker, smoother curve), for a 2% SDS solution. This result, and a similar calculation for the same solution containing 1% PEO, indicates that SDS micelles, which are 5.0 nm in diameter without polymer in solution, are reduced in size to 4.2 nm in diameter when PEO is present. In both cases the thickness of the electron-rich 'corona' was evaluated as 0.6 nm.

In the presence of high concentrations of a strong electrolyte such as NaCl (the system was kept at 40°C to prevent precipitation), SDS forms thread-like ('worm-like', 'cylindrical') micelles[20]. This can be very clearly seen in cryo-TEM images, such as that shown in *Figure 6*. Based on scattering data alone, it is very difficult, however, to establish whether the micelles are spherical or thread-like. This is clearly demonstrated by the similarity of the experimental curves for spheroidal micelles and thread-like micelles shown in *Figure 7*. It has been speculated that the presence of PEO in this system suppresses the spheroidal to thread-like micellar

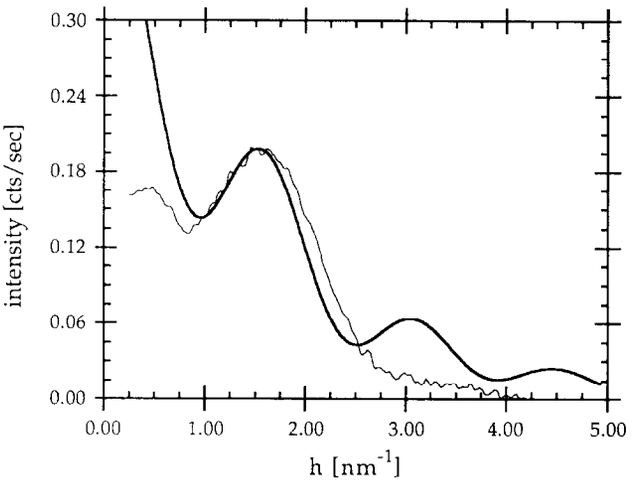

Figure 5 The adjustment of a hollow-sphere form factor with 5.0 nm diameter and 0.6 nm shell thickness to the scattering curve of 2 wt% SDS: model form factor (bold smooth curve); experimental results (thin curve)

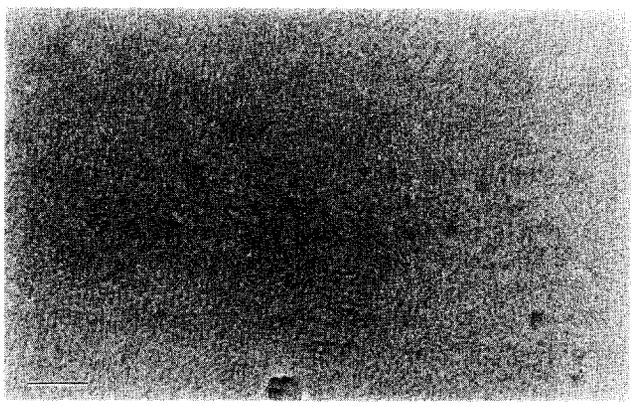

Figure 6 Thread-like micelles observed in a cryo-TEM image of 2 wt% SDS and 0.6 M NaCl solution, vitrified from 40°C (scale bar = 100 nm)

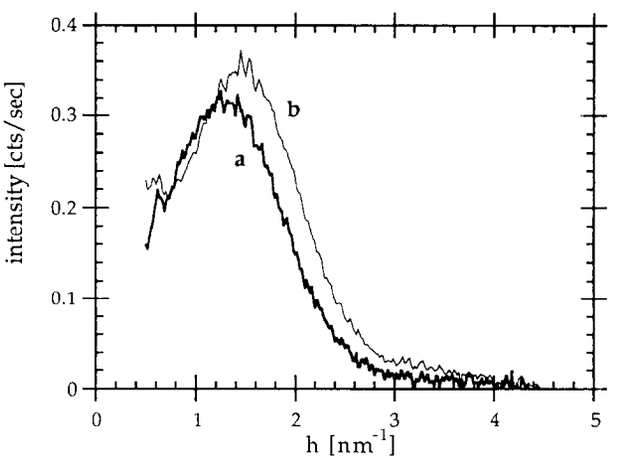

Figure 7 Scattering curves of (a) 2 wt% SDS/0.6 M NaCl (thread-like micelles) and (b) 1.5 wt% PEO/2 wt% SDS/0.6 M NaCl (globular micelles)

transformation upon salt addition[1]. Indeed, our cryo-microscopy work has proven that point beyond any doubt, as demonstrated in *Figure 8*, which shows spheroidal micelles only. Evaluation of micelle diameters from SAXS measurements indicates that the thread-like micelles in solution of 2% SDS with 0.6 or 0.8 M NaCl have a diameter of 6.0 nm. The diameter of the spheroidal micelles obtained upon addition of 1.5% PEO to that system is evaluated as 5.4 nm.

Another issue of interest in this context is the effect of the polymer on the surfactant self-aggregation below the 'normal' (i.e. when no polymer is present in solution) *CMC*. We were able to detect micelles in the PEO/SDS system at 7 mM SDS in the presence of 1% PEO (*Figure 9*), but not below that, owing to the weak signal from the relatively few micelles present at such a low surfactant concentration. Using the hollow-sphere model, a value of 3.8 nm is obtained for the micelle diameter and 0.4 nm for the 'corona' thickness. Both values are significantly smaller than obtained at higher SDS concentrations. Lowering of the *CMC* to a smaller *CAC* is much more pronounced when the affinity of the polymer to surfactant is stronger. We have demonstrated that in the case of SDS and gelatin (a system of much scientific and technological interest in itself). *Figure 10* shows a cryo-TEM micrograph of SDS spheroidal micelles at 5 mM SDS and 1% gelatin. This is also reflected in the strong micellar peak shown in the SAXS data for this system in *Figure 11*. The aggregates that form in this case are found to be 5.0 nm in diameter, with a 'corona' of 0.6 nm, similar to the values obtained for spheroidal micelles in 2% SDS.

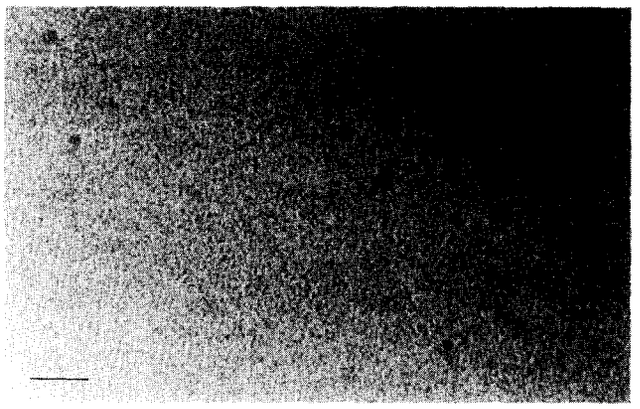

Figure 8 Spheroidal micelles seen in a vitrified cryo-TEM image of 1.5 wt% PEO/2 wt% SDS/0.6 M NaCl solution (scale bar = 100 nm)

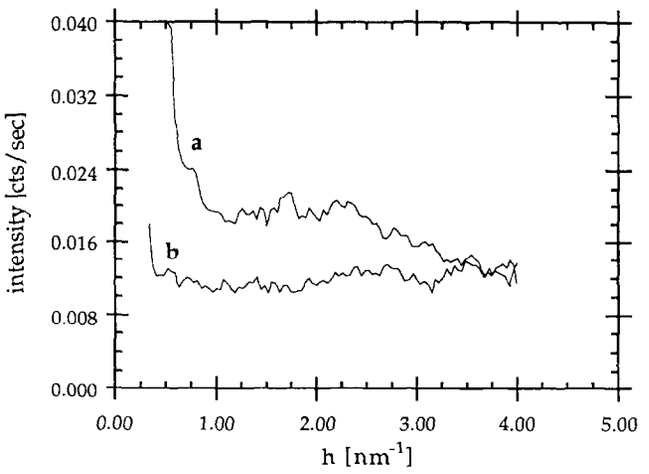

Figure 9 SAXS curves of 7 mM SDS (a) with 1 wt% PEO and (b) without PEO

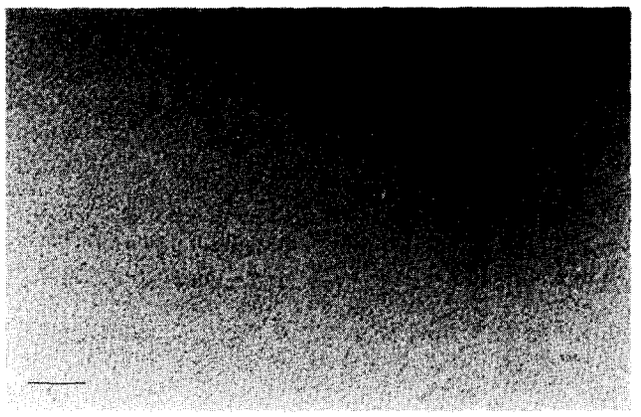

Figure 10 A cryo-TEM image of 5 mM SDS and 1 wt% photographic-grade gelatin: spheroidal micelles are clearly visible (*CMC* of pure SDS is about 8 mM) (scale bar = 100 nm)

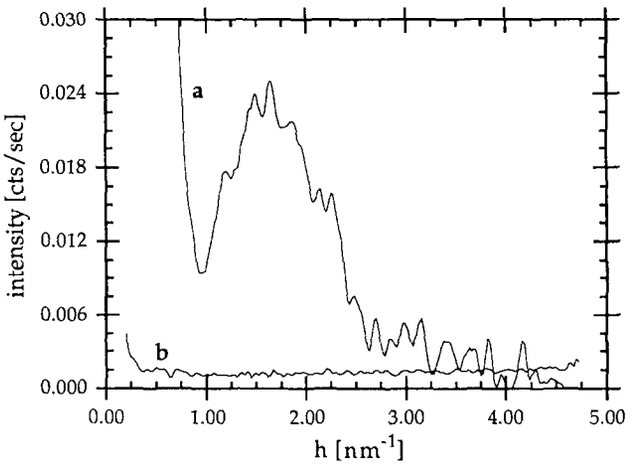

Figure 11 SAXS curves of 5 mM SDS (a) with 1 wt% gelatin and (b) without gelatin

DISCUSSION

The suggested structure of PEO/SDS aggregates was described in detail by Cabane and Duplessix for the dilute[1] and semidilute[21] polymer concentration regimes. A phase diagram was presented for dilute solutions, in terms of polymer and surfactant concentrations. It depicts the critical aggregation concentration (*CAC*) line for surfactant micelles and a stoichiometric ratio of surfactant-to-polymer concentrations for the saturation of PEO with SDS. Within these limits SDS molecules form spherical micelles ('subunits'), bound to the PEO chains, which interact with the micellar surface. This work focuses on the structure of the micellar subunits within the PEO/SDS aggregates. The polymer concentration and molecular weight used in this study yield a semidilute solution well beyond the overlap concentration. Two regions of SDS concentration were studied: dilute solutions near the *CMC*, and concentrated ones near the

stoichiometric PEO/SDS ratio. It is thus assumed that the stoichiometry at saturation can be extrapolated from dilute to semidilute regimes. The main issue addressed in our study is the effect of the polymer on the size and shape of the micellar subunits, at low and high ionic strengths.

Direct observation of SDS micelles by cryo-TEM shows clearly their spheroidal shape in aqueous solution, which is maintained in the PEO/SDS aggregates. It thus provides direct evidence for the model presented by Cabane and Duplessix. At high ionic strength thread-like SDS micelles are imaged for the first time, proving unequivocally the model suggested previously on the basis of changes in the hydrodynamic radius[20] or on rather subtle changes in the observed curves of small-angle neutron scattering[1]. Thread-like micelles had been imaged previously by cryo-TEM in cationic[22], non-ionic[23] and mixed cationic/anionic surfactant systems[24], and in phospholipid/surfactant systems[25]. *Figure 6* exhibits regions of local ordering of the thread-like micelles, but no indication of such local order was given by the scattering patterns. This order is, in all probability, due to the shear induced in the solution during formation of the thin liquid film by blotting during specimen preparation[22].

The size of the micelles cannot be determined accurately by TEM owing to the underfocus of the objective lens needed to obtain sufficient phase contrast for imaging, because of particle overlap, and owing to inaccuracies in instrument magnification. Scattering methods allow a more quantitative evaluation of structural models. SANS measurements[1,17] have the added benefits of contrast variation using deuterated SDS or water, which allows separation of the scattering effects of the polymer and micelles. For the particular issue of evaluating the size and shape of micellar subunits from SANS patterns, calculated curves were fitted to experimental data. The most relevant range of scattering vectors is $1 < h < 2\,\mathrm{nm}^{-1}$. In this range the SANS patterns are monotonically decreasing functions of h, and the most prominent feature to be fitted was a peak obtained when $h^4 I(h)$ was plotted as a function of h. In the same h range SAXS patterns from SDS micelles exhibit a broad peak due to the corona of the electron-rich head-group region of the micelle[17]. The position of this peak is very sensitive to the size of the micelle. Its breadth is influenced by the corona thickness, as well as by polydispersity in the micelle size.

Our results show that the size of ionic micelles can be obtained reliably by fitting the position and breadth of the micellar SAXS peak to a hollow-sphere or -cylinder model, once the shape has been determined by cryo-TEM. In the case of SDS micelles, the decrease in diameter from 5.0 to 4.2 nm in the presence of PEO is clearly indicated by the shift of the position of the scattering peak measured by the readily available SAXS method, as shown in *Figure 4*. However, one must bear in mind the limitations of this procedure. The model does not account for intermicellar interference, which gives rise to a scattering peak at low angles[26], nor does it account for the scattering from PEO. However, both effects are prominent only at low angles and do not much affect the h range of the intramicellar peak. This low h region was also deemed unimportant in the SANS analysis when the data were multiplied[1] by h^4. More serious is the neglect of polydispersity in the size of the micelles, as well as fluctuations in their shape. These have an affect on the first maximum of the micellar form factor, which is not accounted for by our procedure. They also eliminate the oscillations of the form factor at large h, as shown in *Figure 5*. A micellar model of finer detail is best approached by analysis of high-resolution SANS data obtained over a wide angular range under controlled contrast matching conditions, as reported for free SDS micelles[2]. The shape of the micelle should still be verified by direct microscopical observation.

Our evaluation of the effect of PEO on the size and shape of SDS micelles, which corroborates results of several earlier studies, shows that the presence of the polymer induces a higher curvature of the hydrocarbon/water interface and a larger area per surfactant head-group. Thus at the higher SDS concentration studied, interactions with PEO reduce the diameter of the spherical micelles. This effect is more pronounced at low SDS concentration, where the interaction with PEO results in reduction of the *CAC*, and yields spheroidal micelles of much smaller size. At high ionic strength this effect is vividly seen in the electron micrographs, which depict the transformation from cylindrical to spherical shape in the presence of PEO. Several models were suggested for this effect, such as interaction between PEO and the hydrated head-groups[1,9], PEO adsorption at the hydrocarbon/water interface reducing its interfacial energy[27–29], or interaction between PEO and the counterions around the micelle[30]. These models suggest a larger area per surfactant head-group and are thus in agreement with the observed changes in the micellar size and shape upon interaction with PEO. Structural studies by scattering or microscopy techniques cannot distinguish between the different mechanisms.

The effect of the strength of the polymer/surfactant interactions becomes quite clear when the results for PEO/SDS are compared to those of the gelatin/SDS system. That SDS interacts more strongly with gelatin than with PEO is evident from comparing the values of its *CAC*, 0.9 mM in the presence of gelatin[31] and 4.0 mM in the presence of PEO[14]. The size of the micelles we detected by SAXS at 5 mM SDS in the presence of gelatin is comparable to that observed in the PEO/SDS system at much higher concentration, near the saturation limit of the polymer at the same polymer concentration. Since it was shown that the size of the micelles near the *CAC* is smaller than the size they achieve at higher concentrations, this indicates that at 5 mM SDS a significant number of micelles already exist. The present experiments cannot quantify the concentration of those micelles, for lack of an absolute measure of the scattered intensity. However, the prominent intramicellar peak observed at 5 mM SDS in the presence of gelatin, and the micellar size determined from this peak, are an indication for the strength of the gelatin/SDS interactions compared with those in the PEO/SDS system.

ACKNOWLEDGEMENTS

This research was supported in part by grants from the Procter & Gamble Co., Cincinnati, Ohio, and from the Fund for Advancement of Research at the Technion. We would like to thanks Mrs B. Shdemati and Mrs Judith Schmidt for expert technical help.

REFERENCES

1 Cabane, B. and Duplessix, R. *J. Physique* 1982, **43**, 1529
2 Cabane, B. and Duplessix, R. *J. Colloid Surf.* 1985, **13**, 19
3 Lindman, B. and Thalberg, K. in 'Polymer-Surfactant Interactions' (Eds. E. D. Goddard and K. P. Ananthapadmanabhan), CRC Press, Boca Raton, FL, 1993, p. 203
4 Goddard, E. E. *Colloids Surf.* 1986, **19**, 301
5 Illiopoulos, I., Wang, T. K. and Audebert, R. *Langmuir* 1991, **7**, 617
6 Zana, R., Kaplun, A. and Talmon, Y. *Langmuir* 1993, **9**, 1948
7 Burns, J. L., Cohen, Y. and Talmon, Y. *J. Phys. Chem.* 1990, **94**, 5308
8 Shirahama, K. and Ide, N. *J. Colloid Interface Sci.* 1976, **54**, 450
9 Moroi, Y., Akisoda, H., Saito, M. and Matura, R. *J. Colloid Interface Sci.* 1977, **61**, 233
10 Cabane, B. *J. Phys. Chem.* 1977, **81**, 1639
11 Brackman, J. C. *Langmuir* 1991, **7**, 469
12 Jones, M. N. *J. Colloid Interface Sci.* 1967, **23**, 36
13 van Stam, J., Almgren, M. and Lindblad, C. *Prog. Colloid Polym. Sci.* 1991, **84**, 13
14 Zana, R., Lianos, P. and Lang, K. J. *J. Phys. Chem.* 1985, **89**, 41
15 Brackman, J. C. and Engberts, J. B. F. N. *J. Colloid Interface Sci.* 1989, **132**, 250
16 Bellare, J. R., Davis, H. T., Scriven, L. E. and Talmon, Y. *J. Electron Microsc. Tech.* 1988, **10**, 87
17 Zemb, T. and Charpin, P. *J. Physique* 1985, **46**, 249
18 Tardieu, A. and Luzzati, V. *Biochim. Biophys. Acta* 1970, **219**, 11
19 Glatter, O. and Kratky, O. 'Small Angle X-Ray Scattering', Academic Press, London, 1982
20 Mazer, N. A., Benedek, G. B. and Carey, M. C. *J. Phys. Chem.* 1976, **80**, 1075
21 Cabane, B. and Duplessix, R. *J. Physique* 1987, **48**, 651
22 Clausen, T. M., Vinson, P. K., Minter, J. R., Davis, H. T., Talmon, Y. and Miller, W. G. *J. Phys. Chem.* 1992, **96**, 474
23 Lin, Z., Davis, H. T. and Scriven, L. E. *Langmuir* 1992, **8**, 2200
24 Kamenka, N., Chorro, M., Talmon, Y. and Zana, R. *Colloids Surf.* 1992, **67**, 213
25 Walter, A., Vinson, P. K., Kaplun, A. and Talmon, Y. *Biophys. J.* 1991, **60**, 1315
26 Hayter, J. B. and Penfold, J. *J. Chem. Soc. Faraday Trans. (I)* 1981, **77**, 1851
27 Nagarajan, R. *Colloid Surf.* 1985, **13**, 1
28 Ruckenstein, E., Huber, G. and Hoffmann, H. *Langmuir* 1987, **3**, 382
29 Gao, Z., Wasylishem, R. E. and Kawk, J. C. T. *J. Phys. Chem.* 1991, **95**, 462
30 Dublin, P. L., Gruber, J. H., Xia, J. and Zhang, H. *J. Colloid Interface Sci.* 1992, **148**, 35
31 Greener, J., Contestable, B. A. and Bale, M. D. *Macromolecules* 1987, **20**, 2490